Vibrations of strongly irregular or fractal resonators

B. Sapoval and Th. Gobron
Laboratoire de Physique de la Matière Condensée, Ecole Polytechnique, 91128 Palaiseau CEDEX, France
(Received 14 January 1992; revised manuscript received 5 February 1993)

It is shown on a specific example that fractal boundary conditions drastically alter the properties of wave excitations in space. The low-frequency part of the vibration spectrum of a finite-range fractal drum is computed using an analogy between the Helmoltz equation and the diffusion equation. The irregularity of the frontier is found to influence strongly the density of states at low frequency. The fractal perimeter generates a specific screening effect. Very near the frontier, the decrease of the wave form is related directly to the behavior of the harmonic measure. The possibility of localization of the vibrations is qualitatively discussed and we show that localized modes may exist at low frequencies if the geometrical structures possess narrow paths. Possible application of these results to the interpretation of thermal properties of binary glasses is briefly discussed.

PACS number(s): 64.60.Ak, 03.40.Kf, 63.50.+x, 68.35.Ja

INTRODUCTION

Objects with irregular geometry are ubiquitous in nature and their vibrational properties are of general interest. How do trees respond to wind? How do sea waves depend on the topography or geometrical structure of coasts and breakwaters? How can we explain the vibrational properties of glasses? All these questions are largely unanswered. The emergence of the notion of fractal geometry is a significant breakthrough in the description of irregularity [1]. Not only does fractal geometry permit a description of strong statistical irregularity, but it allows us to consider strongly irregular deterministic objects as good approximate objects to understand. If the physical properties of the objects that we consider are in fact related to the hierarchical character of the geometry, then their principal physical characteristics can be found by studying these deterministic objects [2].

Fractal objects have no translational invariance. We know that when a physical system has complete translational invariance it can support wave excitations of any wavelength. When the system has limited translational invariance it can support only a restricted set of excitations. This is true of lattice waves in crystals and of microwave cavities. A fractal object has dilatation invariance but not translational invariance and cannot transmit ordinary waves. The study of waves or harmonic oscillations carried by fractals is a particular case of the study of localization or delocalization of single eigenstates much like the problem of Anderson localization. Here however, "disorder" comes in the form of a geometrical irregularity which can be studied in the approximate deterministic situation. It has already been shown that the excitations of a fractal lattice, called fractons, are generally localized [3,4]. The purpose of the present paper is to present a partial study of the vibrations of an object which is not a fractal object but which is bounded by a fractal boundary. This is the case of a fractal bounded resonator introduced by Berry in the form of a conjecture on the value of the asymptotic density of states [5]. Significant mathematical effort [6–9] has been undertaken, but little has been done in the field of physics because the conjecture [5] predicts a small correction to the density of states, an effect hardly perceptible under the usual physical conditions. For instance, the radiation from a fractal blackbody is expected to be essentially the same as the radiation of an ordinary blackbody. Up to now little has been done to study the structure of the modes of vibrations and their properties [10]. A preliminary experimental and numerical study of the vibrations of a fractal drum has been published recently [11]. In that paper, the experimental observation of localization was attributed to the existence of finite damping.

In addition to the spatial distribution of the harmonic excitations, the two main properties of resonators are their spectrum and their damping. This paper will deal mainly with the first aspect: wave forms, density of states, and possible localization.

To avoid confusion with the fracton problem we propose to call the modes of vibrations of an homogeneous medium bound by the fractal boundary *fractinos*. In order to relate this name to the usual vocabulary of the field of fractals note that fractons are vibrations of mass fractals while fractinos would be vibrations of surface fractals. The last section of this paper presents a proposition for a unified vocabulary for the vibrations of fractal systems.

We consider here the excitations of a fractal drum, or more precisely of a fractal tambourine. We first compute the eigenfrequencies and wave forms using an analogy between the Helmholtz and the diffusion equations. With the diffusion picture one can describe the behavior of the profile of the wave near the boundary and relate it to the harmonic measure on the same frontier. We show that the vibrations exhibit infinite derivatives at some points at the edge of the fractal boundary. The problem of the vibrations localization is qualitatively examined. Localization in a small region of the drum may exist for low-frequency modes if there exists a "narrow path" in the structure of the drum. Finally, we give a brief qualitative

description of how these results may help to understand vibrational properties in binary glasses.

FREQUENCY SPECTRUM AND WAVE FORMS

We have calculated numerically the lowest-energy modes of the fractal drum for different orders of iteration, in the absence of damping. The method, as explained below, is based in the analogy between the wave equation and the diffusion equation. Let V be the interior of the drum and Γ its boundary where the amplitude of the wave Ψ is zero. The free-wave equation, which we wish to solve in the volume (surface) of the fractal drum, is

$$\Delta\Psi=(1/c^2)\frac{\partial^2\Psi}{\partial t^2}\ , \tag{1}$$

where c is the wave velocity, depending on the tension and density of the membrane. Classically, time-factorized solutions of this equation are known to be of the form

$$z(x,y,t)=\Psi(x,y)\exp(i\omega t)\ , \tag{2}$$

where the wave form $\Psi(x,y)$ is a solution of the eigenvalue equation for the Laplacian in the region V:

$$\Delta\Psi=(-\omega^2/c^2)\Psi\ . \tag{3}$$

A direct numerical integration of Eq. (3) is known to possess instabilities. Instead we consider the time-dependent diffusion equation on the same domain V with absorbing boundary conditions:

$$D\Delta\Psi=\frac{\partial\Psi}{\partial t}\ , \tag{4}$$

where D is the diffusion coefficient. Similarly, solutions of the form

$$z(x,y,t)=\Psi(x,y)\exp(-t/\tau) \tag{5}$$

lead to the eigenvalue problem:

$$\Delta\Psi=(-1/D\tau)\Psi\ , \tag{6}$$

and hence also to the wave eigenvalue problem (3) through the correspondence

$$(D\tau)^{-1}=\omega^2/c^2\ . \tag{7}$$

So far this is the same problem, but we can study numerically the time evolution equation (4). We order the set of all the solutions (Ψ_n,τ_n) with decreasing values of τ_n, so that Ψ_n is the eigenfunction associated with the nth mode, with

$$\tau_0\geq\tau_1\geq\tau_2\geq\cdots\geq\tau_n\geq\cdots\ . \tag{8}$$

Now any function $z(x,y)$ defined on V can be expanded on the basis of all eigenvalues Ψ_n as

$$z(x,y)=\sum_n c_n\Psi_n(x,y)\ . \tag{9}$$

Taking this function as an initial distribution $z(x,y,t=0)=z(x,y)$ and computing numerically its time evolution through Eq. (4) will result after a time t in the profile $z(x,y,t)$:

$$z(x,y,t)=\sum_n c_n\exp(-t/\tau_n)\Psi_n(x,y)\ . \tag{10}$$

Equation (10) states that the coefficients of the linear expansion will tend to zero with different time constants τ_n. Hence, except for possible degeneracy, the eigenfunction with the largest time constant and nonzero initial weight will dominate after some time, so that $z(x,y,t)$ becomes a better and better approximation to the fundamental. We start, for example, with a constant trial function $z_0(x,y,t=0)=1$. After a given time the numerical evolution leads to a function proportional to $\Psi_0(x,y)\exp(-t/\tau_0)$. Numerically, this may be verified by looking for the regime when the function $z(x,y,t)$ decays everywhere with the same time constant up to a small predetermined relative error. An example of the decay in time of the average concentration of particles is shown in Fig. 1. At long times the decay is found to be exponential. From the exponential time constant τ_0 we

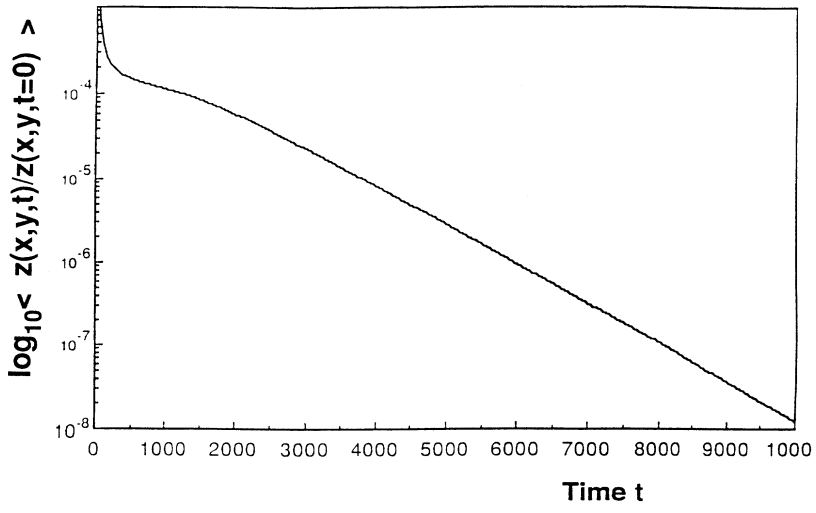

FIG. 1. Decay of the local concentration as a function of time. The long term time constant is τ_0.

find ω_0 using relation (7). We then normalize the waveform function to obtain $\Psi_0(x,y)$. Then the next trial function is

$$z_1(x,y,t=0)=1-\Psi_0(x,y)\int_{\text{drum}}\Psi_0(x,y)ds\ , \qquad (11)$$

which is orthogonal to $\Psi_0(x,y)$. The new distribution converges to the next eigenfunction with nonzero initial weight, namely $\Psi_1(x,y)$. The procedure is then iterated and the states are obtained sequentially, orthogonalizing the $(n+1)$th initial distribution to the n previously computed eigenfunctions, thus converging to the $(n+1)$th one. Such a method cannot be used for an indefinite number of eigenmodes as numerical errors can add up at each step. Of course, for a state to be found in this process it must have a nonzero weight in the initial distribution or appear in the numerical evolution from the numerical noise which has components on any state. The drum possess a C_4 symmetry from which we know that the eigenstates are either conserved through a rotation of $\pi/2$ and π or change sign after a rotation of $\pi/2$ or π. As a consequence we start either with a distribution which is positive in the four quadrants $(+,+,+,+)$ or which is like $(+,-,+,-)$ or $(+,+,-,-)$, corresponding to a state of degeneracy 2 through a rotation of $\pi/2$. We then separate *ab initio* the modes of different symmetry, which as the double interest of giving a better separation between modes (and a smaller time of convergence) and diminishing the number of orthogonalization procedures (and the error propagation accordingly). In the case of degeneracy the algorithm yields a combination of the degenerate modes, depending on the initial profile.

For numerical efficiency, the diffusion equation (3) was discretized both in space and time, so that the computation took place on a square grid compatible with the boundary conditions. To evaluate the quality of our results we must discuss the various sources of uncertainty. There are in principle three types of errors in this method: systematic errors due to time and space discretization and numerical errors due to truncation of numbers in the computation.

Time discretization amounts to the replacement of $\exp(-t/\tau)$ by its discretized form $\exp(-n)(\Delta t/\tau)$ or by $[\exp(-\Delta t/\tau)]^n$, which is a power law. Here Δt is the discretization time interval such that $t=n\Delta t$. This effect does not appear in the results as presented here.

The systematic effect of space discretization can be evaluated by comparison with the case of a square drum for which exact solutions are known both for the continuous and the discretized form. The vibrating modes of the continuous square drum can be labeled by the number of half wavelengths in the x,y directions n and m. The square of the eigenfrequencies is simply given by the sum of their squares. Using a reduced frequency Ω defined by $\Omega=\omega/\omega_0$, where $\omega_0=2^{1/2}\pi c/L$ is the fundamental frequency of the square drum with a side L,

$$\Omega^2(m,n)=(m^2+n^2)/2\ , \quad m,n=1,2,3,\ldots\ . \qquad (12)$$

On a square grid with Z segments per side, the exact formula is [13]

$$\Omega_Z^2(m,n)=(Z^2/\pi^2)[2-\cos(\pi n/Z)-\cos(\pi m/Z)]\ , \qquad (13)$$

which converges to (12) when Z tends to infinity. The systematic error obtained by approximating (12) by (13) is of order

$$\Delta(\Omega^2)=(\Omega^2-\Omega_Z^2)\approx(\pi^2/24Z^2)(m^4+n^4)\ . \qquad (14)$$

As discussed later the number N of states up to Ω^2 is of order $(\pi/2)\Omega^2$. The average distance between two consecutive states is of the order of the inverse of the density of states, i.e., of order $2/\pi$. The systematic error due to the presence of the grid is of the order of two consecutive states separation when

$$(\pi^2/24Z^2)(m^4+n^4)\approx 2/\pi\ . \qquad (15)$$

This condition corresponds to $N\sim 2Z$. We have calculated the eigenvalues in the case of the fractal shown in Fig. 2 for generation $\nu=0$ (the square initiator) with $Z=128$, generation $\nu=1$ and 2 with the same Z, and generation $\nu=3$ with $Z=256$. The number of points on the smaller linear segment of the fractal perimeter is then, respectively, 127, 31, 7 and 3. With the above values of Z we can obtain of the order of 100 states with good accuracy.

Note that what appears as a systematic error due to space discretization in the calculation of the continuous membrane disappears when one consider the harmonic vibrations of a real discretized system. For example, our results are exact (apart from numerical error) for the vibrations of a small fractal crystallite containing Z^2 atoms arranged in the same manner as in our discretized drum.

Apart from the systematic effects of space discretiza-

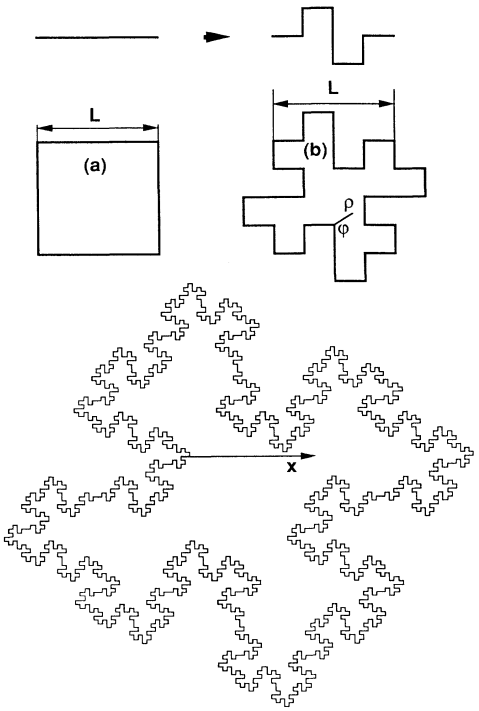

FIG. 2. The fractal drum at stage $\nu=0$, 1, and 3 of iteration. The generator is shown at the top. The area of the vibrating membrane is conserved through the iteration process. The fractal dimension of the perimeter is $D=\ln 8/\ln 4=\frac{3}{2}$.

tion, the errors are due to numerical truncation in the computer. The calculation is performed on a Siemens VP200 vector processor in double precision. As the amplitude of the function decays, the relative error due to number truncation increases. For this reason we take care to renormalize the evolving distribution. Also, as the eigenfunctions are found only with a finite precision, there is always a (small) contribution of the previous states in the starting function. As the process takes place the relative contribution of these states increases because they correspond to a larger time constant. For this reason we take care to regularly reorthogonalize the evolving distribution to the previous states. The final precision is then determined mostly by "how close to an exponential decay" we choose to stop the computation. To characterize quantitatively this accuracy we compare the distributions at different times $z(x,y,t_1)$, $z(x,y,t_2)$, $z(x,y,t_3)\ldots$. We compute the norm of these functions respectively, $N(t_1)$, $N(t_2)$, and $N(T_3)$, ... We then look for the maximum deviation between the renormalized distribution,

$$\begin{aligned} A_{12} &= \max_{x,y} |z(x,y,t_2)/N(t_2) - z(x,y,t_1)/N(t_1)| \ , \\ A_{23} &= \max_{xy} |z(x,y,t_3)/N(t_3) - z(x,y,t_2)/N(t_2)| \ , \\ &\vdots \end{aligned} \tag{16}$$

and wait for these deviations to be smaller than a predetermined deviation δ which we have chosen equal to 10^{-6}. The choice of the parameter δ is in fact a point of some difficulty as it determines the computing time and the computational error, which itself determines the separation of quasidegenerate modes. To calibrate δ we benefited from the results of the square for which we have exact solutions. Of course interference between systematic and numerical mechanisms can perturb the accuracy and it is for this reason that comparison with a known case is of great utility, as we show now.

The average time for the computation of one state is of the order of 10 s for the discretized square 127×127. For a given geometry, computing time grows linearly with the number of points inside the drum. But for the same number of points the computing time (for a given numerical accuracy) depends significantly on the geometry because, as we will see, there can exist regions of the drum which are slow to equilibrate. For example, for the fractal with $\nu=2$ the average time for the computation of one state was of the order of 1 min for the same 127×127 number of inner points. We have computed 300 eigenvalues for the discretized square and the fractal of generation 1, 256 eigenvalues for generation 2, and 100 eigenvalues for generation 3. The results of the computation of the eigenfrequencies are shown in Table I for the 20 lower values [12]. The values of Ω^2 are, respectively, exact values for the continuous square [Eq. (12)], exact values [Eq. (13)] for the discretized square with 127 inner sites per segment, numerical results for the discretized square with 127 sites per segment, the fractal with $\nu=1$ with 31 sites per segment, the fractal with $\nu=2$ with 7 sites per segment, and the fractal with $\nu=3$ with 3 sites per segment. The difference between the continuous and the discretized square is due only to discretization. The comparison between the numerical values obtained for the discretized square and the exact values calculated from Eq. (13) give a qualitative measure for our precision. The largest deviation (of order 10^{-5}) is found for $N=11$, but the average error is much smaller. It is interesting to

TABLE I. Eigenvalues of the Laplacian on various drums (in reduced units). The first column gives the index (or integrated density of states) of the state. The second column gives the exact eigenvalues for the continuous square drum [Eq. (12)]. Column 3 gives the exact results from Eq. (13) for the discretized square with 127 inner sites per segment. Columns 4, 5, 6, and 7 give, respectively, the numerical eigenvalues for generations 0 (the discretized square) and the fractal drums with $\nu=1$, 2, and 3.

Index	$(n^2+m^2)/2$	Eq. (13)	Gen.0	$\nu=1$	$\nu=2$	$\nu=3$
1	1.00	0.999 949 992	0.999 949 992	3.331 800 00	4.135 399 82	4.410 699 84
2	2.50	2.499 573 23	2.499 573 23	6.258 099 08	8.891 093 25	9.812 215 81
3	2.50	2.499 573 23	2.499 573 23	6.258 099 08	8.891 093 25	9.812 215 81
4	4.00	3.999 196 77	3.999 196 77	6.562 184 81	9.216 758 73	10.183 505 1
5	5.00	4.997 941 97	4.997 942 45	6.930 742 26	9.368 745 80	10.305 823 3
6	5.00	4.997 941 97	4.997 942 45	8.748 752 59	10.582 866 7	11.278 085 7
7	6.50	6.497 565 75	6.497 565 75	8.748 752 59	10.582 866 7	11.278 085 7
8	6.50	6.497 565 75	6.497 565 75	11.025 989 5	14.366 231 0	15.410 146 5
9	8.50	8.493 551 25	8.493 551 25	11.896 759 0	16.293 294 9	17.644 975 7
10	8.50	8.493 551 25	8.493 551 25	12.113 400 5	17.165 271 8	18.670 120 2
11	9.00	8.995 934 49	9.995 790 48	12.113 400 5	17.165 271 8	18.670 120 2
12	10.0	9.993 174 55	9.993 175 51	12.420 825 0	18.225 462 0	19.800 184 2
13	10.0	9.993 174 55	9.993 175 51	13.298 184 4	19.440 460 2	20.990 697 9
14	12.5	12.491 543 8	12.491 543 8	14.503 058 4	21.187 755 6	22.624 874 1
15	12.5	12.491 543 8	12.491 543 8	14.503 058 4	21.514 782 0	23.164 888 4
16	13.0	12.984 000 2	12.984 294 9	15.987 000 5	21.514 782 0	23.164 888 4
17	13.0	12.984 295 8	12.984 294 9	17.093 399 0	25.070 900 0	26.946 233 7
18	14.5	14.483 919 1	14.483 918 2	18.239 650 7	25.631 858 8	27.560 514 5
19	14.5	14.483 919 1	14.483 918 2	18.846 210 5	28.059 351 0	30.571 870 8
20	16.0	15.987 153 1	15.987 000 5	18.846 210 5	28.059 351 0	30.571 870 8

note that the state $N=11$ for which the error is maximum is the closest to other states. We are then qualitatively in a situation of quasidegeneracy in which one expects a lower precision. The fact that the numerical errors do not increase for higher frequency is in itself qualitative evidence that the eigenfunctions are obtained with very good accuracy. Even for much higher eigenvalues the numerical precision is very good in the case of the discretized square: for example, the state $n=m=14$ is the state $N=288$. The value from Eq. (13) is $\Omega^2=194.079\,113$ and the numerical value is found to be equal to 194.079 117. For this state the relative numerical error is only of order 3×10^{-9}. It demonstrates that our criterion for convergence is in fact very stringent.

Another test, this one on the fractal itself, uses the fact that the fractal drum at a given order of iteration ν is constituted by a collection of joint identical squares of size $L/4^{\nu}$. Some modes of the fractal drum, which can be considered as "trivial," are compatible with this decomposition and for that reason can be easily computed analytically. In these trivial states an elementary segment of the contour contains an integer number of half wavelengths. The eigenfunctions have the form

$$\psi(x,y)\sim\sin(2^{2\nu}\mu\pi x/L)\sin(2^{2\nu}\mu'\pi y/L)\ , \tag{17}$$

where $\mu,\mu'=1,2,3,\ldots$. The exact eigenvalue corresponding to (17) is

$$\Omega^2=2^{4\nu-1}(\mu^2+\mu'^2)\ . \tag{18}$$

For example, the state $n=m=4$ of the square ($N=20$) corresponds to the state $N=16,\mu=1,\mu'=1$ for the fractal with $\nu=1$. The corresponding numerical eigenvalue found in Table I is good to better than 10^{-9}. Other examples are given in Table II. The deviation between the exact and the numerical values are at most of order 10^{-6} and in most of the cases smaller than 10^{-9}. The larger errors corresponds to states which are quasidegenerate. If the numerical precision was infinite there would be no interest in this comparison because the trivial states are essentially the states on the smaller identical squares which are of the same for the fractal and for the square. However, if significant numerical errors were perturbing the calculation of the nontrivial fractal states that would induce an error in our process in which errors can add, resulting in errors in the final values for the trivial states. The very fact that we find no evidence of numerical errors for the trivial states is an indication that we can have good confidence in our numerical values.

Finally note that our method gives both the eigenfunction and the eigenvalue in the same step and this is true of eigenfunctions which have infinite derivatives at some points on the perimeter as discussed in the next section.

THE WAVE FORM OF THE FUNDAMENTAL

We have concentrated on the study of the density of states and of the geometric properties of the fundamental wave form. We have given special attention to the computation of the wave form of the fundamental state of the drum of generation $\nu=3$ by using a grid with eight lattice spacings for the smaller segment (511×511 points in the drum). A picture of the fundamental is shown in Fig. 3 (top). It exhibits no node line as predicted by general theorems [14] and it is centered in the central part of the drum and corresponds to $\Omega_0=2.1002$ (in our reduced units). One observes in the figure that the amplitude decays strongly from the center towards the edges of the drum. This is exemplified in Fig. 3 (lower part) where the space dependence of the logarithm of the amplitude is shown. The fact that the apparent slope of that "mountain" increases when the deepest bay is reached is a visual indication of the fractal "screening" of the wave form. The spatial dependence of the logarithm of the amplitude along the x direction indicated in Fig. 2 is shown in Fig. 4. There are four regions that we wish to discuss: *A*, *B*, *C*, and *D*.

The very steep increase near the origin (region *A*) is a visualization of the singular behavior of the modes near the wedges of the frontier geometry. Very near the boundary the modes are singular in the sense that their derivatives are infinite at particular points on the frontier [10]. Consider, for example, Fig. 2 in the region of the membrane around a salient corner. Very near the boundary the amplitude of the vibration is very small and

TABLE II. Comparison of the numerical results for the "trivial" states of generation 1 and the corresponding value for the discretized square. Columns 1, 2, and 3 give, respectively, the index (n,m) of a state of the discretized square, its number in the hierarchy of eigenvalues, and the exact eigenvalue given by Eq. (13). Columns 4, 5, and 6 give, respectively, the index (μ,μ'), the number in the hierarchy, and the numerical eigenvalues for the trivial states of the drum with $\nu=1$. The indices (μ,μ') are those appearing in Eq. (17), which gives for the continuous membrane the same value as Eq. (12) for the corresponding values of (n,m).

n	m	$N_{\nu=0}$	$(\Omega_{\nu=0})^2$	μ	μ'	$N_{\nu=1}$	$(\Omega_{\nu=1})^2$
4	8	53(54)	39.890 899 7	1	2	48(49)	39.890 899 7
8	8	90	63.794 647 2	2	2	77	63.794 998 2
4	12	113(114)	79.474 617 0	1	3	105(106)	79.474 617 0
8	12	151(152)	103.378 365	2	3	134(135)	103.378 365
4	16	198(199)	134.357 071	1	4	184(185)	134.357 071
12	12	208	142.962 082	3	3	193	142.962 082
8	16	233(234)	158.260 818	2	4	215(216)	168.260 818
12	16	295(296)	197.844 818	3	4	269(270)	197.844 543

$\Delta\psi \approx 0$. In the polar coordinates (ρ,φ) of Fig. 2 the solution is of the form $\psi \sim \rho^{2/3}\sin(2\varphi/3)$. The derivative $\partial\psi/\partial\rho \sim \rho^{-1/3}$ goes to infinity when ρ goes to 0. This corresponds to a local infinite stress and strain of the membrane. Such a property should be true near equivalent salient points in the structure. If one would have rounded salient wedges, the derivative would not tend to infinity but to a large finite value proportional to the inverse of the radius of curvature of the contour. Singularities of the amplitude around the wedges are apparent in Fig. 3. Should the frontier possess an infinitely sharp edge, the singular modes would have infinite derivatives near the fractal boundaries. In an experiment they would then exhibit infinite stress in the elastic membrane and rupture around these points even for a finite amplitude of excitation. The behavior of the singularity is exemplified in Fig. 5 where a plot of $\log_{10}(\Psi)$ as a function of $\log_{10}(x)$ is shown. The direction x corresponds to $\varphi=\pi$ and $\rho=x$. The slope in Fig. 5 is found to be equal to 0.71 instead of $\frac{2}{3}$, predicted by the above argument. This relatively large difference is probably due to the fact that it is near salient points that discretization has the stronger effects on the numerical wave profile.

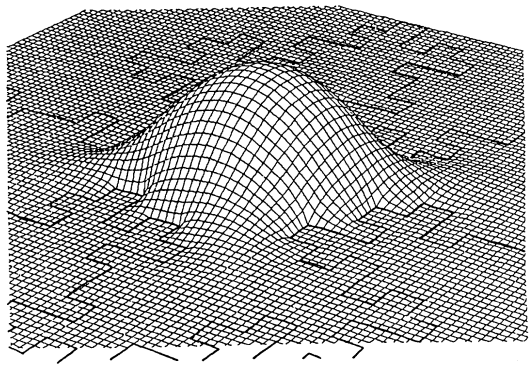

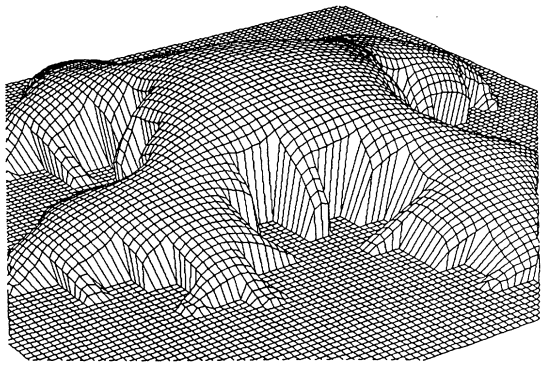

FIG. 3. Wave form of the fundamental vibration for $\nu=3$. Top: the wave form itself. Bottom: the logarithm of the wave form. The fact that the apparent slope of this logarithmic mountain increases when moving towards the narrower and narrower bays is indicative of the screening of the wave by the structure. The derivative of the wave form is very large at salient corners.

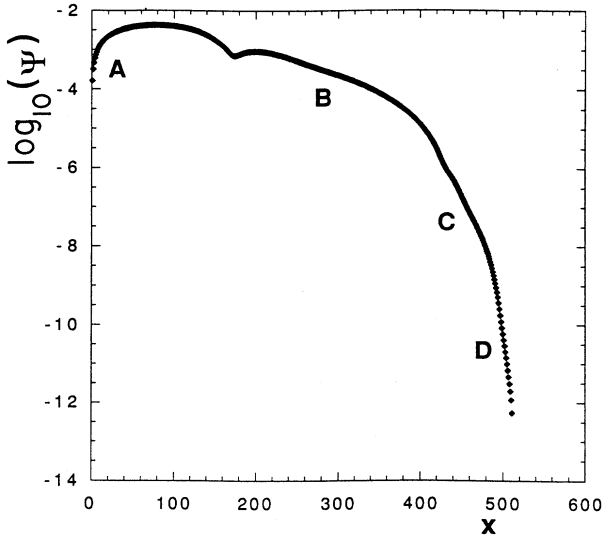

FIG. 4. Space dependence of the fundamental wave form. The logarithm of the amplitude of the fundamental is given as a function of the x coordinate indicated in Fig. 2. In region A near a salient point the wave form exhibits a singular behavior. Note the successive quasilinear decreases of the logarithm in regions B, C, and D.

In regions B, C, and D the behavior can be approximately described by a succession of exponential decays with increasing rapidity. This is qualitatively reminiscent of which has been called "superlocalization" [15]. In the case of superlocalization the spatial dependence is of the form $\Psi \sim \exp(-x^{\alpha})$. Here the screening effect is even more efficient. It is caused qualitatively by the fact that the wave has to penetrate into narrower and narrower channels to get to the frontier.

One can give the following simple argument for the existence of an extremely rapid decrease of the wave ampli-

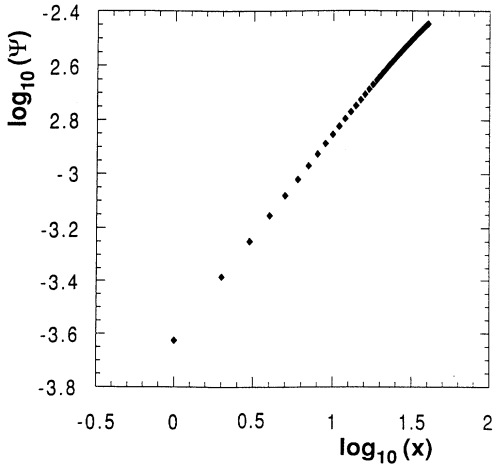

FIG. 5. Singular behavior of the fundamental wave form near a salient corner. The observed slope is 0.71 instead of 0.66 predicted by the behavior of the solutions of the continuous Laplace equation near a salient corner.

tude in smaller and smaller regions of the fractal geometry. This argument is based on the diffusion picture for our problem. We consider the fundamental state which has an exponential decay time τ_0 of the order of L^2/D where L is the macroscopic size of the fractal tambourine. This characteristic time is to be compared with a local diffusion time in a region of the drum with a much smaller characteristic size l. Locally the decay time is of the order of l^2/D much smaller than τ_0. Because we know that the entire wave form decays exponentially with the time constant τ_0, there must exist a mechanism which compensates for the rapid absorption of particles by the nearby frontier. The compensating mechanism can only be diffusion from a broader region. But to compensate for the rapid decay the diffusion flux must be large and this is possible only if the gradient of the concentration (or wave form) is large enough. In other words, the concentration has to vary very rapidly in space.

This indicates that the time-dependent term in Eq. (1) can be neglected in the study of the behavior of the wave near the frontier where the Helmoltz equation reduces to the Laplace equation. Then the knowledge which we have from the study of the harmonic measure and its multifractal distribution can be used to describe the attenuation of the amplitude of the wave [16].

Qualitatively one can consider the variation of ψ in smaller and smaller apertures as in Fig. 6. The value of the concentration of diffusing particles in the region i of typical size L/α^i is ψ_i and ψ_{i+1} in region $i+1$ of size L/α^{i+1}. The rate of absorption of particles by the frontier in region i is of the order of $\psi_{i+1}(L/\alpha^i)^2/D^{-1}(L/\alpha^i)^2$ or $D\psi_{i+1}$. This must be approximately equal to the net diffusion flux which from Fick's law is of order $(L/\alpha^i)D(\psi_i-\psi_{i+1})/(L/\alpha^i)$ or $D(\psi_i-\psi_{i+1})$. Consequently, whatever the consecutive smaller and smaller regions that we consider, the decrease $(\psi_i-\psi_{i+1})$ is of order of ψ_{i+1}. Written as a differential equation, we have on the average $(L/\alpha^i)(d\psi/dx)_{(x=xi)}=-\psi_{(x=xi)}$ or

$$\left[\frac{d\psi}{dx}\right]/\psi\approx -1/w(x)\ , \tag{19}$$

where $w(x)$ is the "local width" of the channel in which we study the wave attenuation. For a parallel slit of constant width $w(x)=a$ the attenuation is proportional to $\exp(-\pi x/a)$ [16].

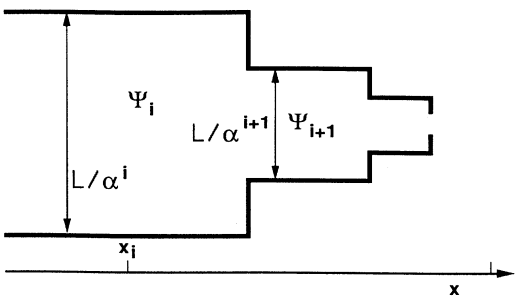

FIG. 6. Behavior of the wave amplitude in narrower and narrower regions.

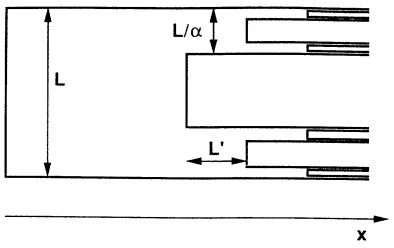

FIG. 7. A Cantor bar screener in which the wave is screened as $\exp(-A^x)$.

Approximating the decay in regions B, C, and D of Fig. 4 by exponentials, the slopes of the logarithmic plot are, respectively, -0.0105, -0.041, and -0.163. These slopes are in a ratio of order 4, clearly compatible with the successive widths in the geometry determined by a dilation factor α equal to 4.

In the same framework one could consider the properties of certain geometries as "wave screeners." For instance, Fig. 7 shows a drum with a Cantor bar frontier. It is merely a succession of narrower and narrower guides of length L' and width a/α^n. After a distance $x=nL'$ along the bar, the amplitude should be of the order of $(a/\Lambda)\alpha^{-n}\exp[-(\pi L'/a)(\alpha+\alpha^2+\cdots+\alpha^n)]$, or in first approximation $(a/\Lambda)\alpha^{-n}\exp[-(\pi L'\alpha^n/a)]=(a/\Lambda)\alpha^{-x/L'}\exp[-(\pi L'\alpha^{x/L'}/a)]$. This is indeed a very rapid decrease of the wave amplitude. It is more rapid than the "superlocalization" behavior. Note that the Cantor bar is not self-similar but self-affine. It is qualitatively clear that the effectiveness for screening in these self-affine structures is higher than in self-similar structures because pores become narrower more rapidly than they become deeper.

The fact that the information dimension of the harmonic measure has a dimension of one in $d=2$ indicates that whatever the roughness of a $d=2$ resonator the frequency of the fundamental will be related to the overall size of the resonator. This could be different in $d=3$ where we do not have general results on the behavior of the harmonic measure.

THE LOW-FREQUENCY DENSITY OF STATES

The question of how the density of states of a resonator depends on its geometry is an old question in mathematical physics (see Refs. [5–9] and references therein) that has been discussed only in the so-called asymptotic limit: Let $N(X)$ denote the counting function (or the integrated density of states) that is the number of eigenvalues (including multiplicity) of the equation $\Delta\Psi=-X\Psi$ smaller than X. Then for a resonator in dimension d and for $X\to\infty$

$$N(X)=(2\pi)^{-d}B_d V_d X^{d/2}+C(X)\ , \tag{20}$$

where B_d is the volume of the unit ball in R_d, V_d is the volume of the resonator (the surface for a membrane), and $C(X)$ is a correcting term, the relative contribution

of which tends to 0 when $X \to \infty$. Recently an expression ha been conjectured for $C(X)$ for a fractal resonator so that the density of states could be written (with our notation)

$$N(\Omega^2)=(\pi/2)\Omega^2-c_{d,D}M(D,\Gamma)\Omega^D + (\text{higher-order terms}) . \quad (21)$$

Here D is the Minkowski dimension of the frontier, $M(D,\Gamma)$ is the Minkowski content of the frontier (the "fractal" equivalent of the length or the surface), and $c_{d,D}$ is a positive constant depending only on d and D. This constitutes the Weyl-Berry-Lapidus [7–9] conjecture which has been demonstrated by Lapidus and Pomerance in the case of $d=1$. This conjecture holds for a real mathematical fractal, that is, for the case where the order of iteration goes to infinity.

Two remarks can be made about the above equation. This formula describes the asymptotic behavior when $\Omega \to \infty$. For a resonator with a fractal frontier, $D<d$ and the fractal contribution is only a correction to the normal density of states. This asymptotic effect then can hardly play a role in the physical properties of a resonator. For instance, a fractal blackbody would radiate essentially like a smooth blackbody. The fact that what appears in formula (20) is the Minkowski dimension is intuitively clear since one expects that the volume of the resonator in the vicinity of the frontier should be able to accommodate a half wavelength.

If we consider now a "physical" fractal with only a finite range of decimation, the above formula tells us that the correction, in the asymptotic limit, is that for a smooth surface. The "gross" fractal structure plays no role in the asymptotic frequency range.

The results of our computation are shown in Fig. 8. The main effect that one finds in Fig. 8 is the marked decrease of the density of states due to the irregularity of the frontier. Increasing the order of the generation has a smaller and smaller effect on a given eigenvalue. Although we are considering in this paper the low-frequency states for which the higher-order terms in Eq. (20) may play an important role, it is interesting to compare Eq. (20) with our results for the frequency range in which we work. The correction $C(\Omega^2)$ due to the surface roughness is the difference between the density of states of the smooth resonator ($\nu=0$) and that in the fractal:

$$C_\nu(\Omega^2)=N(\Omega^2)_{\nu=0}-N(\Omega^2)_\nu , \quad (22)$$

where $N(\Omega^2)_\nu$ is the numerical value of the integrated density of states and $N(\Omega^2)_{\nu=0}$ is calculated for the same values of Ω^2 by a linear interpolation fit. The results are shown in Fig. 9.

The lower curve is the correction term for the drum with $\nu=1$. This drum is irregular, but only for scales larger than $L/4$. If one considers vibrations with half wavelengths smaller than $L/4$, the density of states should be approximately that of an ordinary drum with the same area. It is known that the density of states is of the order of the number of squares with sides equal to a half wavelength, which are necessary to cover the entire surface of a resonator. If one notes that the coordinate Ω^2 represents [from relation (12)] twice the square of the number of wavelengths in the sides of the square, one expects that for n and $m \gg 4$ the density of states is close to that of the smooth resonator with the same area. This is in fact the case as shown in Fig. 9 in which the correction term saturates very quickly for $\Omega^2 > 20$.

For the drum with $\nu=2$ the range of perturbed behavior is extended by a factor 4^2. This corresponds roughly to the range of values that we have calculate. For the drum with $\nu=3$ the number of states that we have calculated is too small to permit comparison. A power-law fit of the correction gives $C(\Omega^2)_{\nu=2} \approx \Omega^{1.26}$ in-

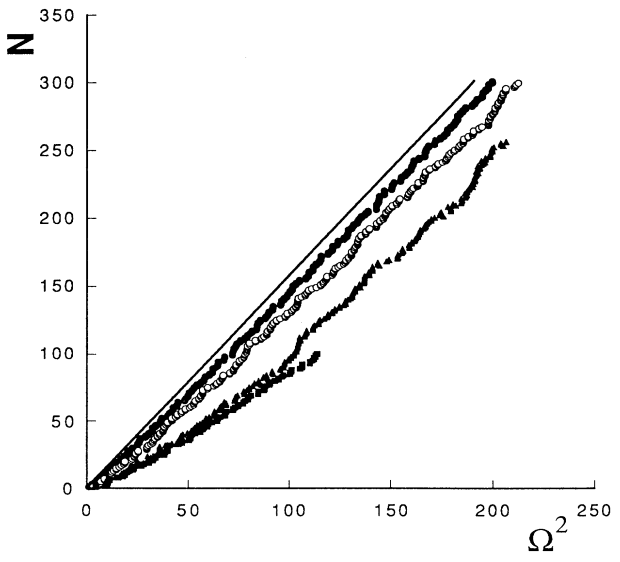

FIG. 8. Integrated density of state $N(\Omega^2)$ as a function of Ω^2 for various orders of decimation of the fractal frontier. From top to bottom: discretized square, fractal drum with $\nu=1$, 2, and 3.

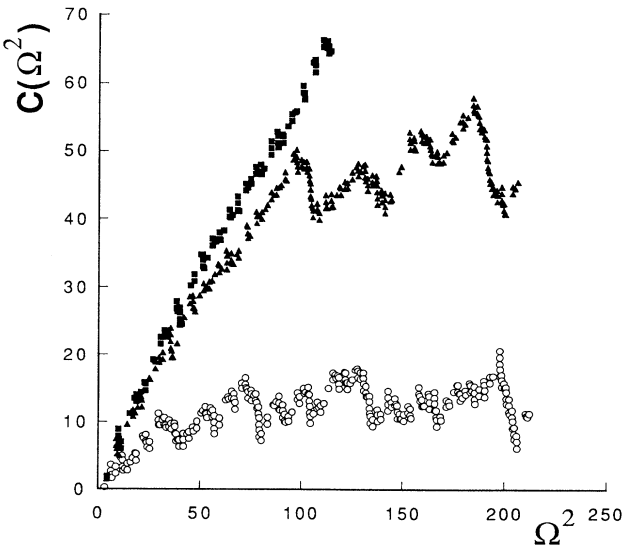

FIG. 9. Correction to the density of states due to the geometry of the frontier. From bottom to top fractal drum with $\nu=1$, 2, and 3.

stead of $\Omega^{1.5}$, predicted by relation (21). This shows that the higher-order terms in Eq. (21) are not totally negligible in this regime.

ARE FRACTINOS LOCALIZED OR NOT?

The problem of localization is a very general problem in the physics of disordered materials and has received considerable attention in the past. Usually the problem is considered in the following context. A disordered system is imbedded in an infinite (or quasi-infinite) medium and the problem is to understand which excitations of the system are localized. A localized state corresponds to a wave form $\psi(r)$, which is essentially contained in a finite volume in contradistinction to a delocalized state which occupies an infinite (or semi-infinite) volume. Here, any vibration is confined in the volume of the resonator and in that sense is trivially localized. But one can still make a distinction between the states depending on how these states fill the internal volume of the resonator. From now on we discuss this property. More precisely, following Thouless, we will call the localization surface (volume) of a given normalized state Ψ the quantity s_l (v_l) defined by

$$s_l = \left[\int |\Psi|^4 ds \right]^{-1} . \tag{23}$$

It is this quantity that we now evaluate for different cases. We consider a very schematic geometry as constituted by a square drum on which a smaller drum is branched as shown in Fig. 10. The larger drum has a side L, the small drum has a side L/α, and they are separated by a "narrow" channel of width a and length Δ. The problem that we address is to what extent a state of the entire system can be localized in the smaller drum. Because wave problems and quantum mechanics have similar formulation [Eq. (3) has the form of the time-independent Schrödinger equation], we will discuss that problem in the content of quantum wells, probably more familiar to the reader. A fractal drum is in this framework a fractal quantum well in $d=2$. To discuss this question we use ordinary Rayleigh perturbation theory and the standard language of quantum mechanics. We keep in mind that the correspondence between an energy E for a quantum particle with mass m and the square of the frequency for the drum is given by

$$\omega^2 = (8\pi^2 mc^2/h^2)E . \tag{24}$$

where h is the Planck constant. We call Ψ_V and Ψ_v the states in the large and small drums, respectively. The energy spectrum of the noninteracting drums is schematized in Fig. 10. In this scheme we wish to find which states of the interacting drums are localized, if any, in the small drum. For simplicity we consider the normalized fundamental state of the smaller drum Ψ_v with energy E_v. In a suitable system of coordinates

$$\Psi_v = 2(\alpha/L)\sin(\pi\alpha x/L)\sin(\pi\alpha y/L) , \tag{25}$$

$$E_v = (h^2/4m)(\alpha/L)^2 . \tag{26}$$

Among the states of the large drum the nearest to E_v is Ψ_V with energy E_V corresponding to some adequate values for n and m

$$\Psi_V = 2L^{-1}\sin(n\pi x/L)\sin(m\pi y/L) , \tag{27}$$

$$E_V = (h^2/8m)L^{-2}(n^2+m^2) . \tag{28}$$

Because $E_v \sim E_V$

$$[(n^2+m^2)/2]^{1/2} \sim \alpha , \tag{29}$$

and in the following we will use for simplicity $n \sim \alpha$. If a channel of width a and length Δ exists as in Fig. 10 there is a small "leak" of both states which permits the interaction. To find this leak we have to find solutions of the Schrödinger equation which in the channel is written

$$(-h^2/8\pi^2 m)\left[\frac{\partial^2\Psi}{\partial x'^2}+\frac{\partial^2\Psi}{\partial y'^2}\right] = K\Psi \approx (h^2/4m)(\alpha/L)^2\Psi \tag{30}$$

because a small aperture will not perturb significantly the energy. Solutions are of the form $\Psi \sim \exp(-kx')\sin(y'\pi/a)$ with

$$k^2-(\pi/a)^2 = 2\pi^2(\alpha/L)^2 . \tag{31}$$

If the channel is "narrow", $a < 2L/\alpha$ and

$$k \approx \pi/a . \tag{32}$$

In first approximation the wave functions in the channel are given by

$$\Psi_v \sim 2a(\alpha/L)^2\exp(-kx')\sin(\pi y'/a) , \tag{33}$$

$$\Psi_V \sim 2a\alpha L^{-2}\exp[k(x'-\Delta)]\sin(\pi y'/a) , \tag{34}$$

where we have taken into account approximatively that the amplitude has to be matched to the oscillations inside the drums. The matrix element of the interaction Hamiltonian, here the kinetic energy K in Eq. (30) is easily calculated

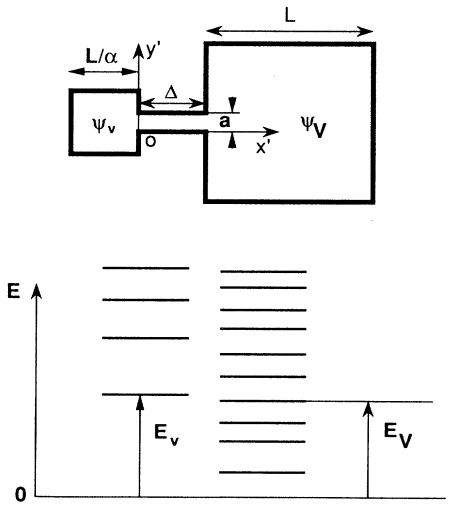

FIG. 10. Scheme of the mechanism of localization of fractinos. Top: geometrical situation. Bottom: scheme of the energy levels comparing the energies in a large resonator to the energy of the fundamental vibration in a smaller region.

$$\langle \Psi_v | K | \Psi_V \rangle \sim (h^2/2m)(\alpha^5 a^3 \Delta / L^6) \exp(-\pi\Delta/a) , \quad (35)$$

where we have used (31)–(34). The first-order perturbed wave function is of the form

$$\Psi_v' = \Psi_v + \epsilon \Psi_V , \quad (36)$$

where ϵ is the contamination factor $\epsilon = \langle \Psi_v | K | \Psi_V \rangle / (E_v - E_V)$. The distance $E_v - E_V$ is, except in the case of resonance, of the order of the distance between consecutive energy level of the large drum (multiplied by $\frac{1}{4}$ on the average). This last quantity is of the order of $(h^2/8\pi m)L^{-2}$ and the order of magnitude of ϵ is

$$\epsilon \sim 4\pi(\alpha^5 a^3 \Delta / L^4) \exp(-\pi\Delta/a) . \quad (37)$$

Under many conditions this factor will be very small and in such a case the perturbed state is localized because

$$s_l = \left[\int |\Psi_v + \epsilon \Psi_V|^4 ds \right]^{-1} \approx (L/\alpha)^2 \quad (38)$$

and the localization surface is essentially that of the smaller drum. When one considers states which are higher in the spectrum, this localization property will disappear because the matrix elements of the interaction increases. However, in $d=2$ this localization property is really a hierarchical property since if one considers a situation in which a smaller resonator is connected to the above two, the same reasoning will apply and there will also exist states which are localized in this smaller cavity. The conclusion is that in such a situation in $d=2$, there may exist an infinity of localized states, of course provided that there exists "narrow channels" in the drum geometry. The existence of states localized at the edge will depend on how ramified the edge region is, and therefore depends on the fractal dimension of the boundary. Even more, with the same fractal dimension, localization will be favored by the presence of these narrow channels.

In principle, similar results could be obtained in $d=3$, but in $d=3$ the energy levels are more and more dense at high energy and the "contamination factor" increases. In consequence, in $d=3$, only states at low energy can be localized (again if narrow channels exist). In both $d=2$ and 3 the localized states are a small fraction of the total number of states at high energy.

FRACTONS, SURFACE FRACTONS, AND FRACTINOS IN BINARY GLASSES

We discuss now why we found it necessary to introduce the term *fractinos* to name the vibrations of a fractal tambourine. We propose a unified vocabulary to avoid confusion in future discussion. One must start from the general term of fractal resonator to describe a resonator with fractal geometry. This term was introduced by Berry [5]. There are two kinds of fractal resonators: mass fractal resonators and surface fractal resonators. The first case to be studied has been the case of the harmonic vibrations of mass fractals and were named fractons. This term is appropriate since in several cases the vibrations of mass fractal have a density of states characterized by a spectral dimension very different from the Euclidian dimension and the fractal dimension [3,4]. Also these fractons have special localizations properties. Note that all vibrations of mass fractals do not have necessarily all these properties, but it seems reasonable to keep the name of fractons to describe the vibrations of mass fractals.

Coming to the vibrations of surface fractals, one could think of the term of *surface fractons* to name these vibrations (keeping in mind that usual fractons could be considered as "mass fractons"). Unfortunately, this would be misleading in three ways. First the name *surface fracton* intuitively describes the vibrations of the outer surface of an object, much like the name *surface phonons* describes the vibrations of the surface (or the region very near the surface) of crystals. Here the surface itself is fixed and does not vibrate. Second, as we have seen above, the density of states for the vibrations of surface fractals is very different from that of fractons. Even more important, there can exist real surface fractons which are vibrations of the fractal surface of an object and which have the properties of ordinary (mass) fractons. The name *surface fractons* should be reserved to describe the vibrational properties of these fractal interfaces. A known example of fractal interface is a diffusion front and we give below an example of the possible existence of interface fractons in an otherwise dense Euclidian material. It is then because surface fractons can really exist that one cannot use this term to name the vibrations of surface fractals which are studied in this paper. It is for this very reason that a new word is necessary and that we propose the term of *fractino.*

A physical situation in which both fractinos and surface fractons could be observed would be the case of a Euclidian solid which could be considered as a collection of fractal drums. Consider, for instance, an A,B solid which has the structure shown in Fig. 11. In such a system the distribution of mass is nonfractal, but there exists

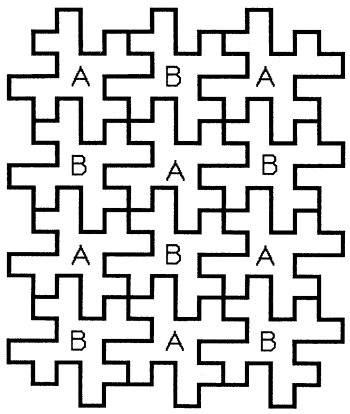

FIG. 11. A dense material with fractal internal interfaces. The system as shown is periodic, but if randomized it could give an image of an amorphous binary A-B system after phase separation. In the case where the A atoms are joined together by very soft springs the vibrations of the A atoms could be fractinos while the vibrations of the interfaces could be fractons.

in the solid an array of fractal internal interfaces. If the local vibrational properties of A and B are strongly contrasted (for example, if the A-A springs are very soft and the B-B springs very hard), it is possible that the A-A vibrations behave approximately as fractinos and that the vibrations of A-B interfaces possess the properties of fractons. The fact that internal interfaces can be mass fractal was shown several years ago, when it was shown that diffusion fronts are natural mass fractals [17]. A schematic picture of a diffusion front is shown in Fig. 12. A diffusion front is essentially the outer edge of a percolation cluster. In $d=3$ it is a mass fractal which could very well exhibit fracton dynamics.

Such structure and dynamics may be the clue of the observation of fractons in the dynamics of dense binary amorphous materials. Raman and neutron inelastic scattering of the mixed superionic glasses such as the silver iodide, silver borate binary compounds of general composition $(AgI)_x(Ag_2O\cdot B_2O_3)_{1-x}$ have been interpreted using the fracton concept but without a picture of what is really fractal in this material [18].

We propose the following qualitative explanation for these experimental observations. Such a material is an interconnected network of AgI and $(Ag_2O\cdot B_2O_3)$ regions of small scale. Because it is prepared from cooling from the melt, it could present fractal interfaces between the regions of different nature [17]. This material being the glass which possess the highest known ionic conductivity, the silver ions or part of the silver ions are weakly coupled to the cage. They can possibly be the A atoms which are coupled together by very soft springs. The low-energy spectrum in the neutron scattering data should be then the region where silver-silver fractinos could be observed. As we have seen, the effective density of states in small and rough microcrystalline atomic arrangements could be significantly reduced as compared to smooth microcrystals. The density of states of these fractinos should be smaller than the ω^2 density of states for ordinary phonons, similar to what we have found here. This is effectively what is seen in the Fig. 6 of Ref. [18].

At higher energy one could observe the vibrations of those ions from the case which are at the interface with the silver conducting regions. If these interfaces are fractal, the fracton spectrum which was found in Ref. [18] would correspond to the specific vibrations of the internal fractal interfaces. Note that if the disorder is at small scale, the number of modes associated with the internal interfaces is not negligible. For instance, a cubic microcrystal with a side of ten lattice units has approximately the same number of atoms on its surface than in the bulk. Hence the total number of surface modes is of the same order as the total number of modes of vibrations from the bulk. A characteristic crossover length of 20–30 Å is typically found in these structure as a transition between phonons (fractinos) and fractons [19]. Higher-energy vibrations would correspond in that picture to the B—B vibrations in Fig. 11. Here it could be the B—O the O—I and I—O vibrations. Of course, for this explanation to be feasible one must have a strong contrast between the coupling constants of different atoms a case which is realized in the superionic binary materials. The singular behavior of the vibrations at the salient edges would appear in a comparatively strong anharmonicity of the vibrations a fact which is considered to be necessary to understand the thermal conduction of glasses at moderate temperature [20].

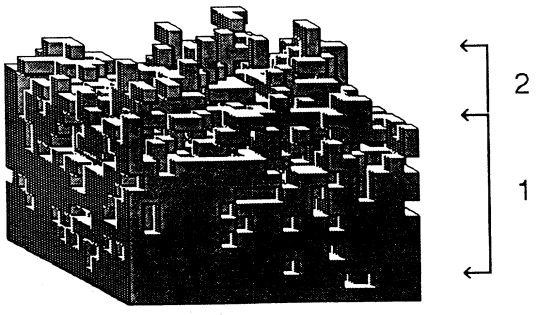

FIG. 12. A diffusion front in $d=3$. Only one kind of atom, for example, the B atom, has been represented for clarity. The upper part of this front is a mass fractal analogous to the percolating cluster, with a fractal dimension of approximately 2.5. If the B-B springs are much harder than the A-A springs the vibrations of this object, which is the interface between A and B can naturally be surface fractons.

CONCLUSION

We have studied, on a specific example, the low-frequency vibrations of a physical fractal drum that we called *fractinos* by computing the spectrum and the wave form of the fundamental. Some of our results are to be considered as indicative of the properties of strongly irregular resonators and some properties are really related to the scaling behavior of the frontier.

The four specific properties of fractinos are a very strong attenuation inside the successive regions of the frontier, a significant reduction of the low-frequency density of states, a singular behavior at salient points, and possible existence of vibrational states which are localized in a small region of the resonator.

The attenuation is a scaling effect which could be described in the standard multifractal framework. This is general to fractal frontiers. In particular the distribution of the stress of the membrane along the frontier should be multifractal. The limited range of our computation was not sufficient to test this result, but the analogy between solutions of the wave and Laplace equation is here to sustain this fact.

The other characteristics are more a property of irregular resonators. If the geometrical structure possess narrow paths, localized states may exist at low frequency. This property will depend intimately of the geometry of the frontier.

Further studies of these systems should include the case of $3d$ resonators and the study of the properties of the resonances in the case where the vibration is free at the boundary, that is the case of von Neuman instead of Dirichlet boundary conditions. The numerical method that we have used has proved to be surprisingly good. It is certainly promising since it can probably be improved by using hierarchical mesh. One most important prob-

lem for future study is the discussion of the damping properties of fractal resonators.

ACKNOWLEDGMENTS

The authors gratefully acknowledge valuable discussions with J. N. Chazalveil, M. Lapidus, A. Margolina, B. Mandelbrot, and J. Peyrière. L. Börjesson, M. Lapidus, and R. Orbach have kindly provided us with their manuscripts prior to publication. Laboratoire de Physique de la Matière Condensée is "Unité de Recherche Associée du Centre National de la Recherche Scientifique No. 1254."

[1] B. B. Mandelbrot, *The Fractal Geometry of Nature* (Freeman, San Francisco, 1982).
[2] B. Sapoval, *Fractals* (Aditech, Paris, 1990).
[3] S. Alexander and R. Orbach, J. Phys. (Paris) Lett. **43**, L625 (1982).
[4] R. Rammal and G. Toulouse, J. Phys. (Paris) Lett. **44**, L13 (1983).
[5] M. V. Berry, in *Structural Stability in Physics,* edited by W. Guttinger and H. Elkeimer (Springer-Verlag, Berlin, 1979), pp. 51–53.
[6] J. Brossard and R. Carmona, Commun. Math. Phys. **104**, 103 (1986).
[7] M. L. Lapidus and J. Fleckinger-Pellé, C. R. Acad. Sci. **306**, I171 (1988).
[8] M. L. Lapidus and H. Maier, C. R. Acad. Sci. **313**, I19 (1991), and references therein.
[9] M. L. Lapidus, Trans. Am. Math. Soc. **323**, 465 (1991), and references therein.
[10] B. Sapoval, Physica D **38**, 296 (1989).
[11] B. Sapoval, Th. Gobron, and A. Margolina, Phys. Rev. Lett. **67**, 2974 (1991).
[12] Tables giving the ensemble of our results are available upon request to the first author.
[13] C. Kittel, *Introduction to Solid State Physics* (Wiley, New York, 1976).
[14] D. Courant and D. Hilbert, *Methods of Mathematical Physics* (Interscience, New York, 1965), Chap. 6.
[15] A. Aharony and A. Brooks Harris, Physica (Amsterdam) **163A**, 38 (1990).
[16] C. J. G. Evertz, P. W. Jones, and B. Mandelbrot, J. Phys. A **24**, 1889 (1990).
[17] B. Sapoval, M. Rosso, and J.-F. Gouyet, in *The Fractal Approach to Heterogeneous Chemistry,* edited by D. Avnir (Wiley, New York, 1989), p. 227, and references therein.
[18] A. Fontana, F. Rocca, M. P. Fontana, B. Rosi, and A. J. Dianoux, Phys. Rev. B **41**, 3778 (1990).
[19] L. Börjesson, R. L. McGreevy, and W. S. Howells, in Fourth International Workshop on Disordered Systems, Andalo, (Trento) Italy 1991 [Philos. Mag. B **65**, 261 (1992)].
[20] R. Orbach, in Fourth International Workshop on Disordered Systems (Ref. [19]), p. 289.